



55th Annual Midwest Student Biomedical Research Forum

Saturday, March 2, 2024

AFTERNOON POSTERS – Ahmanson Ballroom C

P-004

COFILIN: A NOVEL REGULATOR OF BREAST CANCER BRAIN METASTASIS

Presenter: Laiba Anwar, UNMC

P-008

KAWASAKI DISEASE CLINICAL PATHWAY IMPLEMENTATION

Presenter: Bridget Backer, UNMC

P-010

PIPERLONGUMINE DERIVATIVES PROTECT AGAINST AMINOGLYCOSIDE-INDUCED OTOTOXICITY IN ZEBRAFISH

Presenter: Meghna Basavaraju, Creighton University

P-014

MOLECULAR DYNAMICS SIMULATION OF BINDING CHLOROTOXIN FRAGMENTS TO MATRIX METALLOPROTEINASE-2

Presenter: Eli Blaney, Creighton University

P-015

CHARACTERIZING A CLINICALLY RELEVANT TOBRAMYCIN MODEL FOR VESTIBULAR DYSFUNCTION

Presenter: Alyssa Burd, Creighton University

P-016

ϕ, ψ DIHEDRAL SPACE WITHIN THE PROTEIN DATABANK EXPANDED CONFORMATIONS

Presenter: William Burns, Health Partners Institute/Park Nicollet

P-017

ANTIBODY RESPONSES TO CITRULLINATED TYPE II COLLAGEN AND VIMENTIN MODIFIED WITH MALONDIALDEHYDE-ACETALDEHYDE DIFFER IN RHEUMATOID ARTHRITIS AND RHEUMATOID ARTHRITIS-ASSOCIATED INTERSTITIAL LUNG DISEASE

Presenter: Breanna Butler, UNMC

P-018

DEFINE THE NEGATIVE REGULATION OF PR55A EXPRESSION BY P53-CONTROLLED FBXL20/SCF E3 UBIQUITIN LIGASE COMPLEX

Presenter: Alison Camero, UNMC

P-019

DIET QUALITY IN A MIDWESTERN BREAST CANCER COHORT

Presenter: Sarah Carlson, UNMC

COFILIN: A NOVEL REGULATOR OF BREAST CANCER BRAIN METASTASIS

Laiba Anwar¹, Mohammad Abbas Zaidi¹, Aatiya Ahmad¹, Asad Ur Rehman¹, Parvez Khan¹, Mahek Fatima¹, Md Arafat Khan¹, Juan A. Santamaria-Barria², Surinder K Batra^{1,3,4}, Zahoor Shah⁵, Mohd Wasim Nasser^{1,4*}

¹Department of Biochemistry and Molecular Biology, ²Department of Surgery, University of Nebraska Medical Center, Omaha, NE 68108, USA, ³Fred and Pamela Buffett Cancer Center, University of Nebraska Medical Center, Omaha, NE-68198, USA. ⁴Eppley Institute for Research in Cancer and Allied Diseases, University of Nebraska Medical Center, Omaha, NE-68198, USA. ⁵Department of Medicinal and Biological Chemistry, The University of Toledo, 3000 Arlington Avenue, Toledo, OH 43614, USA.

Breast cancer (BC) is the most frequent malignancy in women that shows high rates of distant metastasis. The central nervous system/brain is one of the most common sites of BC metastasis, which is a leading cause of BC-associated mortality, poor prognosis, and low overall survival. The lack of knowledge about the mechanism or modulators of brain metastasis is a major hurdle for developing effective therapies against breast cancer brain metastasis (BCBrM). To better understand the mechanism and key molecules regulating BCBrM, we used a bioinformatics approach for the comparative analysis of RNA seq data from matched primary BC and brain metastatic samples. We found that the gene encoding cofilin-1 was significantly upregulated in BCBrM tissues. Cofilin-1 belongs to actin-binding protein and plays a crucial role in cell movement. It has been shown that increased levels of active cofilin in cancer cells promote metastasis by facilitating epithelial-to-mesenchymal transition, cytoskeletal reorganization, as well as lamellipodium formation. Further, to validate the outcomes of RNA seq data; we performed cofilin expression studies in a panel of BC brain metastatic cell lines and observed substantially high expression of active cofilin in brain metastatic BC cells compared to respective primary cell lines. To block cofilin activity in BCBrM, we synthesized and developed a novel small molecule inhibitor against cofilin that shows superior blood-brain barrier permeability and effectively inhibits the metastatic potential of BC brain metastatic cells. Taken together, our studies suggest that cofilin is a viable target for BCBrM, and cofilin inhibitors have a high potential for developing innovative therapeutic strategies against breast cancer brain metastasis.

EHD1-MEDIATED REGULATION OF MICROTUBULE DYNAMICS IN PRIMARY CILIOGENESIS

Bazella Ashraf, Shuwei Xie, Naava Naslavsky, Steve Caplan

Department of Biochemistry and Molecular Biology, University of Nebraska Medical Center, Omaha NE 68198

Background: The primary cilium is an immotile, microtubule-based sensory organelle that can arise from the mother centriole (m-centriole) during the G0/G1 phase in almost every cell type. A key event in this crucial process is the removal of the capping protein, CP110, from the m-centriole. CP110 undergoes proteasomal degradation upon ubiquitination by the E3-Ub ligase HERC2, which is delivered via microtubule-based transport of centriolar satellites, a process reliant on the function of the endocytic regulatory protein, EHD1. Depletion of EHD1 prevents primary ciliogenesis, whilst compromising centriolar satellite movement. However, the precise mechanism by which EHD1 might regulate the centriolar satellite movement to the m-centriole is still unclear.

Significance of Problem: The sensory roles of the primary cilium are critical to normal homeostasis and development, owing to which defects in the process of ciliogenesis lead to a variety of diseases (ciliopathies), including cancer. Interestingly, a mutation in EHD1 also leads to a form of ciliopathy. Thus, elucidating the mechanism of EHD1-mediated regulation of centriolar satellite movement can greatly inform our understanding of these diseases and help unveil therapeutic targets. It could also reveal a new function for EHD1 as a microtubule-associated protein.

Hypothesis: Based on the manifest effects EHD1 depletion has on the localization and movement of centriolar satellites, we hypothesize that EHD1 regulates microtubule dynamics to control centriolar satellite movement and promote primary ciliogenesis.

Experimental Design: To explore the effect of EHD1 on microtubule dynamics, we exposed mock- and EHD1-siRNA treated HeLa cells to nocodazole for 30-40 minutes to depolymerize microtubules, followed by a washout to allow for microtubule recovery. The cells were then fixed and stained for alpha tubulin, and microtubule recovery was assessed by measuring the radius of the microtubule extension from the centrosome in individual cells. This was repeated with normal parental and EHD1^{-/-} mouse embryonic fibroblast (MEF) cells. Next, to investigate the potential interaction between EHD1 and microtubules, coimmunoprecipitation between EHD1 and tubulins (α , β 1, β 3, and γ) was done in HeLa and retinal pigmented epithelial (RPE-1) cells. To verify the possibility of direct interaction and identify domains involved, GST-EHD1 fusion proteins (including GST attached to the EH domain only) were prepared, for use in an in-vitro microtubule binding assay.

Results: Our results show that the knockout of EHD1 in MEF and HeLa cells impedes microtubule regrowth after nocodazole-induced depolymerization. Additionally, we identified novel interactions between EHD1 and the predominant tubulins which constitute microtubules: α , β 1, β 3, and γ , in HeLa and RPE-1 cells.

Conclusions: Our observations of tubulin-EHD1 interactions and the effect of EHD1 on microtubule dynamics suggest a role in microtubule regulation, which in turn controls centriolar satellite movement required for ciliogenesis. Further studies are aimed at dissecting EHD1-microtubule interactions and understanding precisely how EHD1 factors in microtubule regulation to influence primary ciliogenesis, which may be crucial for understanding how EHD1 mutations lead to ciliopathy.

**PIPERLONGUMINE DERIVATIVES PROTECT AGAINST AMINOGLYCOSIDE-
INDUCED OTOTOXICITY IN ZEBRAFISH**

Dr. Marisa Zallocchi, Meghna Basavaraju

Creighton University – Omaha, Nebraska

Background. Hearing loss is a major health concern in our society, affecting over 400 million people worldwide. Among the causes, aminoglycoside therapy can result in permanent hearing loss in 40-60% of treated patients and despite these high numbers, no drug has yet been approved by the Food and Drug Administration. We have previously conducted a high-throughput screening of bioactive compounds, employing zebrafish as our discovery platform, and identified piperlongumine, an alkaloid extracted from the long pepper *Piper Longum L.*, as an important therapeutic molecule for aminoglycoside-induced hair cell death.

Hypothesis. Improving piperlongumine's efficacy and potency by medicinal chemistry will result in a more effective therapy against aminoglycoside-induced hearing loss.

Material and Methods. Five to six days post-fertilization (dpf) zebrafish are incubated with different concentrations of the piperlongumine derivatives in the presence or absence of kanamycin. Fish are fixed and immunostained with the hair cell marker, otoferlin. The number of hair cells per neuromast is quantified under a fluorescent microscope.

Results. Of the 30 piperlongumine derivatives synthesized by medicinal chemistry, we tested six at four different concentrations. Two of those derivatives, PG-3 and PG-4, showed protection at at least one concentration. The number of neuromast hair cells was significantly higher compared to animals treated with kanamycin alone. Moreover, PG-3 and PG-4 alone at the highest concentration did not result in any general toxicity.

Conclusions and future directions. Piperlongumine derivatives showed an improvement in efficacy and potency as well as low toxicity. Once we finish with the screening of the rest of the derivatives, the top candidate will be moved forward to the next step: the assessment of its therapeutic potential in a more relevant model for aminoglycoside-induced hearing loss.

MOLECULAR DYNAMICS SIMULATION OF BINDING CHLOROTOXIN FRAGMENTS TO MATRIX METALLOPROTEINASE-2

Eli Blaney, Tobin Shea, Charles Watts*, Sándor Lovas

Department of Biomedical Sciences, School of Medicine, Creighton University, Omaha, NE 68178

*Department of Neurosurgery, Park Nicollet, Methodist Hospital, St. Louis Park, MN 55426

Aggressive tumors such as glioblastoma aberrantly express matrix metalloproteinase-2 (MMP-2) to facilitate tissue invasion. Combined with its other behaviors, this expression in patients, leads to a poor prognosis and survival rates. Therefore, effective inhibition of MMP-2 is a desirable target for treatments of this extremely deadly brain cancer. Since MMP inhibitors in use have variable effectiveness in clinical settings, interest is focused on exploring drug candidates that may exhibit more consistent antitumor activity. Chlorotoxin (Ctx) polypeptide from the scorpion (*Leiurus quinquestriatus quinquestriatus*) interacts with human MMP-2 (Othman *et. al.*, 2016). Although, conflicting data exists regarding its inhibitory activity against MMP-2 (Farkas *et. al.*, 2023). Due to the lack of a crystallized structure of MMP-2 – Ctx complex, we employed three molecular docking methodologies followed by molecular dynamics (MD) simulations to find consensus binding and calculate the binding energy of these peptide ligands to MMP-2. Our *hypothesis* is that the C-terminal binding motif of Ctx is responsible for MMP-2 inhibition.

In addition to the Ctx itself, four peptide fragments were chosen for study from various segments at its C-terminal regions: Ac[Ser³⁵,Cyc(28,33)]Ctx(24-36)-NH₂ (P75); Ac-[Cys²⁶,Ser^{28,33},Cyc(26,35)]Ctx(24-36)-NH₂ (P76); Ac-[Cys²⁴,Ser^{28,33},Cyc(24,35)] (P77), and Ac[Cyc(28,33)]Ctx(27-34)-NH₂ (P78). Ctx and its fragments were submitted to molecular docking using HPEPDOCK (HP), HADDOCK (HD), and AlphaFold2 (AF2) methods. Top five poses from each docking approach were submitted to 100 ns MD simulation using the GROMACS software package and the CHARMM36m force field. To select the lowest energy complexes for further MD simulations, the last 50 ps of each trajectory were rescored with the Molecular Mechanics Poisson-Boltzmann Surface Area (MM-PBSA) method. The resultant top models were submitted to a 500 ns MD simulation. Structural stability of complexes and convergence of simulations were determined by calculating root-mean square deviation (RMSD) and conformational entropy. Peptide binding on region of MMP-2 and the final binding energies (ΔE_b) using the MM-PBSA method (last 100 ps of each simulation) were also determined.

Conformational entropy calculations showed that all trajectories converged. RMSD analyses of trajectories showed stable peptide-protein complexes during the 500 ns simulation for each of the peptides. Ctx and its peptide fragments from each docking method frequently bound to regions on MMP-2 other than the catalytic site such as the collagenase-1 and hemopexin-like regions. All three docking methods showed large negative ΔE_b indicating favorable interaction between Ctx and its analogs with MMP-2. Using the three docking methods, Ctx had the following binding energies: $\Delta E_{b, HP} = -62.53 \pm 7.2$ kcal/mol, $\Delta E_{b, AF2} = -53.02 \pm 11.3$ kcal/mol, $\Delta E_{b, HD} = -37.82 \pm 7.9$ kcal/mol. P75 had similarly large binding energies: $\Delta E_{b, HP} = -61.65 \pm 6.7$ kcal/mol, $\Delta E_{b, AF2} = -58.49 \pm 10.3$ kcal/mol and $\Delta E_{b, HD} = -21.80 \pm 6.9$ kcal/mol. P76 binding energies were calculated to be: $\Delta E_{b, HD} = -52.16 \pm 7.3$ kcal/mol, $\Delta E_{b, AF2} = -51.85 \pm 9.3$ kcal/mol, and $\Delta E_{b, HP} = -50.72 \pm 9.6$ kcal/mol. P77 binding energies were: $\Delta E_{b, AF2} = -72.89 \pm 11.2$ kcal/mol, $\Delta E_{b, HP} = -37.59 \pm 10.0$ kcal/mol, and $\Delta E_{b, HD} = -27.78 \pm 6.5$ kcal/mol. Finally, P78 binding energies were: $\Delta E_{b, HP} = -51.72 \pm 6.4$ kcal/mol, $\Delta E_{b, HD} = -41.90 \pm 5.4$ kcal/mol, and $\Delta E_{b, AF2} = -29.94 \pm 11.0$ kcal/mol. Except for P76 and P77, complexes obtained with HP docking had the greatest binding energies. Except for P76 and P78, complexes obtained with HD docking had the weakest binding energies. Among the peptide fragments, the strongest binder to MMP-2 was P75 using the HP method, P76 using the HD method, and P77 using the AF2 method.

Analysis of the simulations show that there is consensus about Ctx and its C-terminal analogs binding to MMP-2. Interactions with the collagenase-1 and hemopexin-like regions of MMP-2 may suggest an allosteric inhibition of its activity. To confirm our *in silico* results, enzyme inhibitory activity *in vitro* and cell migration inhibition *in vivo* against glioblastoma cell lines will be determined.

References:

- Othman, H. *et al. J.Biomol. Struct. and Dyn.* **2016**, 35 (13), 2815–2829.
 Farkas, S. *et al. J.Biological Chemistry.* **2023**, 299 (9), 104998–104998.

CHARACTERIZING A CLINICALLY RELEVANT TOBRAMYCIN MODEL FOR VESTIBULAR DYSFUNCTION

Alyssa Burd¹, Nicole Rud¹, Jonathan Fleegel¹, Sarath Vijayakumar¹

1. Creighton University School of Medicine, Omaha, NE.

Background:

Aminoglycosides, such as tobramycin (TM), are an essential class of antibiotics used to treat a variety of gram negative and positive bacterial infections. While these antibiotics are beneficial against drug-resistant bacteria, these drugs are associated with serious and often irreversible side effects such as hearing loss and vestibular dysfunction. Although, research has been conducted to investigate ototoxic effects of aminoglycosides on hearing loss, little has been done regarding detrimental effects on the vestibular system.

Significance of Problem:

The ototoxic effects of tobramycin on the vestibular system are a current area of research that is understudied and crucial to understand for future diagnosis/prevention. In cystic fibrosis (CF) patients, tobramycin is commonly used to combat infections. Currently, the primary mode for monitoring tobramycin ototoxicity is through hearing evaluations. However, a recent analysis investigating auditory and vestibular function with cystic fibrosis, found that 79% of the patients reported vestibular dysfunction and only 23% had hearing loss. This finding indicates that there may be a significant number of CF patients with vestibular dysfunction that are unidentified and whose needs are unaddressed. This gap in knowledge not only impacts patients' quality of life but poses a threat for future economic costs to them and society for the remainder of their lives. If left unaddressed, these complications will likely become co-morbidities in future years.

Hypothesis:

We hypothesized that mice treated with tobramycin would demonstrate significant vestibular dysfunction, measured by increased vestibular sensory-evoked potential (VsEP) thresholds.

Experimental Design:

For this experiment, Cdh23 strain mice at 10-12 weeks old were treated with tobramycin and/or liposaccharide (LPS) at low and moderate amounts. LPS was used to most accurately replicate conditions of CF patients. The mice were split into five experimental groups: TM only, TM + LPS (low), TM + LPS (moderate), LPS (low) only, and LPS (moderate) only as well as an age-matched control group. LPS was administered via intraperitoneal injection one day prior to starting the two-week tobramycin dosing and two additional times during the two-week period. Tobramycin was administered twice daily via subcutaneous injection for two weeks. Vestibular function was assessed using VsEP three weeks after completion of TM +/- LPS protocol.

Results/Data:

It was found that animals treated with TM + LPS (low) and TM + LPS (moderate) experiment groups had significantly elevated VsEP thresholds compared to the age-matched control group. Threshold was also elevated in the TM only group. No significant differences were observed in the other groups.

Conclusion:

This study demonstrated the negative effect of tobramycin on vestibular function. Animals treated with TM + LPS (low), TM + LPS (moderate), and TM only had a significant elevation in thresholds measured by VsEP. Results from this study emphasize the need to continue investigation of aminoglycoside-induced vestibular dysfunction and prevention.

ϕ, ψ DIHEDRAL SPACE WITHIN THE PROTEIN DATABANK WITH EXPANDED CONFORMATIONS.

William A. Burns¹, Sándor Lovas², Charles R. Watts³

- 1 Health Partners Institute, Bloomington, Minnesota, USA, 55425;
- 2 Department of Biomedical Sciences, Creighton University, Omaha, Nebraska, USA, 68178;
- 3 Department of Neurosurgery, Park Nicollet, Methodist Hospital, St. Louis Park, Minnesota, USA, 55426;

The field of structural biology has exploded in the past decade. With the increasing availability of experimental methods (X-ray diffraction, NMR spectroscopy and electron microscopy) combined with the democratization of computational resources there are >200,000 experimental structures and >1,000,000 computed structural models available within the Protein Databank (PDB).[1] In the Critical Assessment of Techniques for Protein Structure Prediction (CASP13) competition AlphaFold, an artificial intelligence (AI) protein structure prediction method placed first in 2018. [2] The expansion of AI techniques promises to eventually make the structural biology of every known genome available for analysis and design. The implications for understanding physiology and pathology at the molecular level and designer therapy are, therefore staggering. Despite the promise of computational models, the utilization of experimentally solved structures is critical for AI training and quality assurance. Critical components of protein secondary structure are the ϕ, ψ backbone dihedral angles which determine the β , α , α_L , ϵ , and contiguous secondary structure regions. Understanding the propensity of each amino acid for each secondary structure region as well as the mean \pm standard deviation of the associated ϕ, ψ dihedral angles is important information for these models. This information can also be used to refine deterministic techniques such as molecular mechanics and dynamics algorithms to ensure computational accuracy.

Herein we present results of a comprehensive survey and analysis of the ϕ, ψ dihedral angle space within the PDB [1]. PDB (www.rcsb.org) was queried for all experimental protein structures with less than 20 to 25% sequence similarity, resolution 0.5 to 2.5 Å inclusive. The number of non-hydrogen atoms per structure was <60,000 secondary to software restrictions. All non-protein atoms were removed from the structures. Non-proteinogenic amino acids were converted to their nearest equivalent. Structures were relaxed using the Rosetta relaxation method to resolve poor contacts.[3] The explored conformational space of each relaxed protein structure was then expanded by treating the structure as a group of distance and geometric restraints and calculating new structures using tConcoord which operates without forcefield restrictions or potential bias.[4] Conformational expansion ensured that each amino acid had a minimum of 100,000 sampled ϕ, ψ dihedral angles for the analysis. The incidence of each amino acid within the PDB was tabulated. The backbone root-mean-square-deviation (RMSD) for each protein and its generated conformations was used to determine structural validity (RMSD > 2.0 nm from the Rosetta relaxed conformation were rejected). Dihedral angles were extracted from the conformations using Biopython scripts.[5] Regions of β , α , α_L , ϵ , and contiguous dihedral angle space were assigned using density clustering and adherence to the ϕ, ψ dihedral population density maps calculated using the method of Lovell et al.[6]

The results demonstrate that the ϕ, ψ dihedral space of each amino acid within the PDB has an individual and unique population density map with associated propensities for occupying the β , α , α_L , ϵ , and contiguous regions and unique mean \pm standard deviations for the dihedral angles. These properties may play an important role in protein dynamics, folding and conformation and should help with further model development.

References:

1. wwPDB, consortium authors. Protein Data Bank: the single global archive for 3D macromolecular structure data. *Nucleic Acids Research J.* 2018; 47: 520-528. DOI: 10.1093/nar/gky949.
2. Moulton, J.; Pedersen, J. T.; Judson, R.; Fidelis, K. A large-scale experiment to assess protein structure prediction methods. *Proteins: Structure, Function, and Bioinformatics J.* 1995; 23: ii-iv. DOI: 10.1002/prot.340230303
3. Conway, P.; Tyka, M. D.; DiMaio, F.; Kondering, D. E.; Baker, D. Relaxation of backbone bond geometry improves protein energy landscape modeling. 2014; 23: 47-55. DOI: 10.1002/pro.2389.
4. Seeliger, D.; Haas, J.; de Groot, B. L. Geometry-Based Sampling of Conformational Transitions in Proteins. *Structure L.* 2007; 1482-1492. DOI: 10.1016/j.str.2007.09.017.
5. Cock, P. J. A.; Antao, T.; Chang, J. T.; Chapman, B. A.; Cox, C. J.; Dalke, A.; Friedberg, I.; Hamelryck, T.; Kauff, F.; Wilczynski, B. Biopython: freely available Python tools for computational molecular biology and bioinformatics. *Bioinformatics J.* 2009; 25: 1422-1423. DOI: 10.1093/bioinformatics/btp163
6. Lovell, S. C.; Davis, I. W.; Arendall, W. B.; de Bakker, P. I.; Word, J. M.; Prisant, M. G.; Richardson, J. S.; Richardson, D. C. Structure validation by C-alpha geometry: phi,psi and C-beta deviation. *Proteins J.* 2003; 50: 437-450. DOI: 10.1002/prot.10286.

Butler, B

ANTIBODY RESPONSES TO CITRULLINATED TYPE II COLLAGEN AND VIMENTIN MODIFIED WITH MALONDIALDEHYDE-ACETALDEHYDE DIFFER IN RHEUMATOID ARTHRITIS AND RHEUMATOID ARTHRITIS-ASSOCIATED INTERSTITIAL LUNG DISEASE

Breanna M. Butler¹, Jill A. Poole^{2,3}, Michael J. Duryee^{1,3}, Nozima Aripova¹, Carlos D. Hunter^{1,3}, Bridget Kramer^{1,3}, James R. O'Dell^{1,3}, Geoffrey M. Thiele^{1,3}, Bryant R. England^{1,3} and Ted R. Mikuls^{1,3}

¹Department of Internal Medicine, Division of Rheumatology, University of Nebraska Medical Center, Omaha, NE, USA

²Department of Internal Medicine, Division of Allergy, University of Nebraska Medical Center, Omaha, NE, USA

³Veterans Affairs Nebraska-Western Iowa Health Care System, Omaha, NE, USA

Background: Malondialdehyde-acetaldehyde (MAA) adducts are post-translational modifications of arginine residues on proteins and are a product of oxidative stress associated with loss of tolerance in many disease states. We have previously shown that patients with rheumatoid arthritis-associated interstitial lung disease (RA-ILD) had increased levels of serum IgA and IgM antibodies against human serum albumin modified with MAA in addition to having higher levels of anti-citrullinated protein antibodies (ACPA). Moreover, lung tissues from RA-ILD patients demonstrated increased levels of MAA antigen that co-localized with citrullinated (CIT) proteins, Type II Collagen (CII) and Vimentin (VIM), suggesting that MAA may act as a cofactor that increases the immunogenicity of CIT proteins in RA-ILD patients. Therefore, antibody responses to dually modified (MAA and CIT) VIM or CII were evaluated as biomarker(s) to differentiate RA-ILD from RA and idiopathic pulmonary fibrosis (IPF), a condition with marked histopathologic similarities to RA-ILD.

Significance of Problem: Interstitial lung disease (ILD) causes significant complications and mortality in patients with rheumatoid arthritis (RA). Furthermore, very little is known about biomarkers that can predict incident ILD in patients with RA.

Hypothesis: Circulating antibodies against dually modified (MAA and CIT) CII or VIM can serve as potential biomarkers to differentiate RA from RA-ILD.

Experimental Design: Serum was collected from patients with RA, RA-ILD, or IPF (n=15 for each group). All patients with RA fulfilled the 1987 ACR classification criteria. The presence of RA-ILD was confirmed by a board-certified subspecialist (pulmonologist or rheumatologist) and the presence of supportive chest computed tomography (CT) findings. Patients were defined as having RA without ILD in the absence of a clinical diagnosis of ILD or past chest imaging findings suggestive of ILD. All patients with IPF without underlying autoimmune disease were diagnosed by a board-certified pulmonologist and had confirmatory findings of usual interstitial pneumonia (UIP) by chest CT imaging. Samples were assessed for CCP and relative units of IgG, IgM, and IgA antibody levels to CII-MAA-CIT and VIM-MAA-CIT via ELISA. Data was analyzed using a one-way ANOVA with Tukey's multiple comparison test.

Results/Data: Participant characteristics were similar across groups: overall mean age 73 years, 90% male, 87% reporting White race and 68.9% current or former smokers. There was no difference in CCP positivity between RA and RA-ILD patients. Serum IgG antibodies to CII-MAA-CIT were significantly increased in RA-ILD patients compared to RA patients (4-fold higher, $p < 0.05$) and IPF patients (42.5-fold higher, $p < 0.01$) (**Fig. 1A**). Serum IgM (**Fig. 1B**) and IgA (**Fig. 1C**) antibodies to CII-MAA-CIT showed similar trends with IgG anti-CII-MAA-CIT, but only differences in RA-ILD vs. IPF reached statistical significance ($p < 0.05$). In contrast, serum IgG antibodies to VIM-MAA-CIT were significantly increased in RA patients when compared to those with RA-ILD (2-fold higher, $p < 0.05$) and IPF patients (2.1-fold higher, $p < 0.05$) (**Fig. 1D**). Serum IgM (**Fig. 1E**) and IgA (**Fig. 1F**) antibodies to VIM-MAA-CIT showed a similar pattern to IgG anti-VIM-MAA-CIT, but again only differences between RA and IPF reached significance ($p < 0.05$).

Conclusions: Serum IgG antibody levels to dually-modified CII-MAA-CIT and VIM-MAA-CIT differ between patients with RA and RA-ILD. These findings suggest that dual modifications of type II collagen, but not vimentin, generate autoimmune responses that are substantially enhanced in RA-ILD and that could play a role in the pathogenesis of this extra-articular complication.

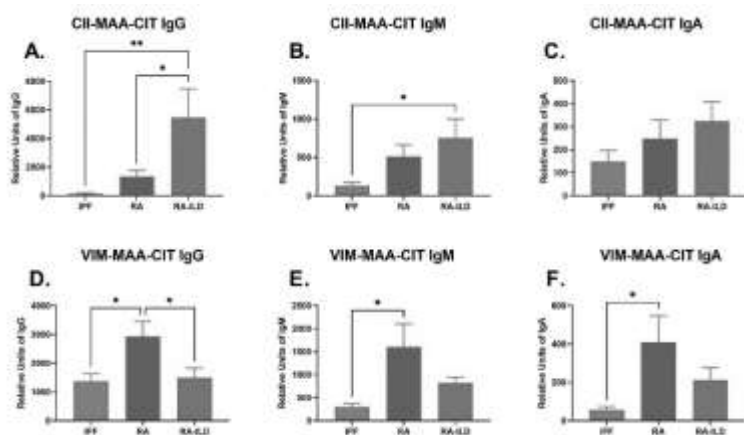


Figure 1. Serum Ig Antibody Levels to Dually Modified Type II Collagen or Vimentin. Samples were assayed by ELISA for (A,D) human IgG (B,E) human IgM (C,F) human IgA. Antibodies to native Collagen and Vimentin were subtracted from MAA-CIT responses. Serum IgG antibodies to CII-MAA-CIT were significantly increased in RA-ILD patients compared to RA patients ($*p < 0.05$) and IPF patients ($**p < 0.01$). Similar trends were observed with IgM and IgA antibodies to CII-MAA-CIT, but only IgM in RA-ILD compared to IPF was significantly increased ($*p < 0.05$). Serum IgG antibodies to VIM-MAA-CIT were significantly increased in RA patients compared to both RA-ILD and IPF patients ($*p < 0.05$). Similar trends were observed with IgM and IgA antibodies to VIM-MAA-CIT, but only RA compared to IPF patients had significantly increased IgM and IgA antibodies ($*p < 0.05$).

DEFINE THE NEGATIVE REGULATION OF PR55A EXPRESSION BY P53-CONTROLLED FBXL20/SCF E3 UBIQUITIN LIGASE COMPLEX

^{1,2}Alison L. Camero, ¹Chitra Palanivel, ³Michel M. Ouellette, and ¹Ying Yan

¹Department of Radiation Oncology; ²Department of Genetics, Cell Biology, and Anatomy; ³Department of Internal Medicine; University of Nebraska Medical Center, Omaha, Nebraska

Background: Pancreatic cancer is among the deadliest cancers in the United States with an overall five-year survival rate of only 12% in 2023. The aggressive nature of the disease, late-stage detection, the limited effectiveness of current treatments, and the lack of targeted therapies all together contribute to its high mortality rate. Previous studies from our lab have identified PR55 α , a regulatory subunit of protein phosphatase 2A (PP2A), playing an essential role in pancreatic cancer development and progression, which is by the support of the hyper-activity of multiple core pancreatic cancer-promoting pathways including YAP, c-Myc, β -catenin, and ERK. Furthermore, recent studies from our lab have discovered a novel pathway by which p53 tumor suppressor controlled FBXL20, a substrate adaptor of an SCF ubiquitin E3 ligase complex, negatively regulates PR55 α protein stability via ubiquitin-mediated proteasomal degradation. These findings have established PR55 α /PP2A as a critical promoter of pancreatic cancer and a potential therapeutic target for pancreatic cancer.

Significance of Problem: Although the p53/FBXL20 pathway has been identified as the negative regulator of PR55 α protein stability, the precise molecular mechanism underlying this regulation remains unknown. Given the great opportunity of developing PR55 α -based targeting therapies for pancreatic cancer, there is a critical need to understand how FBXL20/SCF mediates PR55 α degradation, which includes identifying the binding motifs between FBXL20 and PR55 α , the FBXL20-targeted ubiquitination sites in PR55 α and the additional members of the SCF complex involved in the regulation. A clear understanding of this mechanism can potentially lead to the development of PR55 α -targeted therapeutics for pancreatic cancer treatment.

Question: This project aims to define a novel mechanism by which the FBXL20/SCF E3 ligase complex promotes the proteasomal degradation of PR55 α .

Experimental Design: PR55 α consists of seven WD40 repeats, which are versatile motifs that contribute significantly to its protein-protein interactions, structural stability, substrate recognition and targeting, and isoform specificity. A series of PR55 α truncates were generated by PCR using specific primers designed to target various regions of PR55 α to include and overlap the different WD40 repeats in PR55 α . Subsequently, both the PR55 α truncates and the pWZL-Flag retroviral vector were restriction digested with Mfe1 and Mlu1 endonuclease to create sequence-compatible ends to allow for the ligation of the Flag-B55 α truncates into the pWZL-Flag vector. After ligation and transformation, the plasmid DNAs were isolated from ampicillin-resistant colonies and validated for the presence of the PR55 α truncates by sequencing.

Results/Data: We have successfully generated the seven truncates of PR55 α , cloned them into the pWZL-Flag retroviral vector, and validated their sequences in the vector. These seven truncates, with each including at least two of the seven WD40 domains of PR55 α , can now be expressed as Flag-tagged proteins in mammalian cells for functionality tests.

Ongoing Studies: To attain the goal of this project, Phoenix A 293T cells were transfected with different pWZL-FLAG-PR55 α fragments, with a full-length PR55 α as a positive control, to generate retroviruses, which subsequently were used to infect pancreatic normal and cancer cells to establish stable expressing cells with Blasticidin selection. In the next step, co-immunoprecipitation and immunoblotting techniques will be utilized to further determine the interaction relationships between PR55 α and FBXL20 to identify the smallest functional motif (degron) required for the binding of PR55 α to FBXL20. Functionality tests will validate the identified PR55 α -degron in mediating the degradation of PR55 α by the FBXL20/SCF E3 ligase.

Conclusions: The goal of this study is to identify the binding motif of PR55 α that interacts with FBXL20. This binding interaction is required for the p53/FBXL20 cascade to negatively regulate PR55 α levels by ubiquitination and degradation. Understanding the specifics of this pathway can help advance drug development efforts, honing in on the specific ubiquitination sites of PR55 α . This research bears significant relevance in the realm of pancreatic cancer, a field that is currently limited by few therapeutic options. This study lays the groundwork for a potential breakthrough intervention. We will continue to explore and elucidate the broader functions of the binding motif and its impact on cancer development and progression.

DIET QUALITY IN A MIDWESTERN BREAST CANCER COHORT

Sarah Carlson, Birgit Khanalavala, Jenenne Geske, University of Nebraska Medical Center, Omaha, NE

Background:

Diet quality refers to the measurement of the quality and variety of the diet as a whole. It evaluates whole foods, not just nutrients, and thus allows us to identify relationships between whole foods and health outcomes. Diet quality is scored based on how closely a person follows national dietary guidelines. Many researchers have demonstrated that diet quality impacts cardiovascular risk; the lower the diet quality the higher the cardiovascular disease (CVD) risk becomes. The Rapid Eating Assessment for Participants – shortened version (REAP-S) is a validated way to assess diet quality as it relates to the U.S. Dietary Guidelines. This survey is also recommended by the American Heart Association for clinicians to use to evaluate diet quality and CVD risk. There are limited data regarding the overall diet quality, as it relates to a healthy United States-style diet, in patients who have breast cancer.

Significance of Problem:

Breast cancer is the second most common cancer among U.S. women. Five to ten percent of breast cancer diagnoses are linked to genetic changes, indicating that lifestyle-based risk factors – physical inactivity, nutrition, and overweight/obesity – play a role in a large portion of breast cancer cases, especially in post-menopausal women. This indicates the need for more research surrounding how lifestyle, such as diet quality, might be used to treat, to increase survival after cancer, and to prevent breast cancer. Until we can identify the baseline diet quality of breast cancer patients, we cannot identify areas for change or accurately describe long-term changes made to the diet.

Hypothesis, Problem, or Question:

What is the diet quality, as assessed by the REAP-S, of patients with breast cancer in the Midwest?

Experimental Design:

This cross-sectional study used the REAP-S, a validated nutrition survey to assess diet quality in English-speaking people who have been diagnosed with breast cancer or ductal carcinoma in situ (DCIS) presenting to a midwestern academic medical center. The surveys were scored; higher scores indicate better diet quality.

Results/Data:

The average age of our sample was 60.53 (SD=10.8) years old, and the average BMI was 30.0 (SD=7.2). The mean REAP-S diet quality score for our patient population was 28.44 (SD=4.1) on a scale from 13-39. The low score in our sample was 20 and the high score was 39.

Conclusions:

Although there are not published REAP-S scores for the average American, our average is in range with several other studies that have assessed diet quality in different patient populations including a bipolar adult population (mean of 27.6) and a population of patients seeking bariatric surgery (mean of 28.32). A study of healthy young adults following three basic dietary patterns – omnivorous, vegetarian, and vegan – found that the omnivore population had an average REAP-S score of 31.8, vegetarians averaged 32.7 and vegans averaged 36.1. The diet quality in a Midwest cohort of breast cancer patients was suboptimal.